# THE UNIVERSITY OF RHODE ISLAND

Department of Electrical, Computer, and Biomedical Engineering Faculty Publications

## University of Rhode Island
## DigitalCommons@URI

Department of Electrical, Computer, and Biomedical Engineering

2013

# Using Both GPS L1 C/A and L1C: Strategies to Improve Acquisition Sensitivity

Kelly C. Seals

William R. Michalson

*See next page for additional authors*

Follow this and additional works at: https://digitalcommons.uri.edu/ele_facpubs

**Authors**

Kelly C. Seals, William R. Michalson, Peter F. Swaszek, and Richard J. Hartnett

# Using Both GPS L1 C/A and L1C:
# Strategies to Improve Acquisition Sensitivity

Kelly C. Seals, *U.S. Coast Guard Academy*
William R. Michalson, *Worcester Polytechnic Institute*
Peter F. Swaszek, *University of Rhode Island*
Richard J. Hartnett, *U.S. Coast Guard Academy*

## BIOGRAPHIES

Kelly C. Seals is a member of the Electrical Engineering faculty at the U.S. Coast Guard Academy in New London, Connecticut, and a Ph.D. student at Worcester Polytechnic Institute.

William R. Michalson is a Professor in the ECE Department at the Worcester Polytechnic Institute where he performs research and teaches in the areas of navigation, communications and computer system design. He supervises the WPI Center for Advanced Integrated Radio Navigation (CAIRN).

Peter F. Swaszek is a Professor in the Department of Electrical, Computer, and Biomedical Engineering at the University of Rhode Island. His research interests are in statistical signal processing with a focus on digital communications and electronic navigation systems.

Richard J. Hartnett is a Professor in Electrical Engineering at the U.S. Coast Guard Academy. His research interests include efficient digital filtering techniques for electronic navigation systems and autonomous ground vehicle design.

## ABSTRACT

The upper L-Band will be the only frequency band with two different GPS civil signals available to users at the same carrier frequency with the legacy L1 C/A code signal and the new L1C signal. The null-to-null bandwidth of the C/A code signal is 2.046 MHz. The TMBOC modulation of the L1C signal creates bandwidth of 4.092 MHz between the outer nulls of the largest spectral lobes in the split-spectrum signal. Without the need to have two separate radio-frequency chains in the front-end of a GPS receiver, using the GPS C/A and L1C signals will improve acquisition sensitivity with limited additional complexity.

This paper explores various techniques for joint acquisition of GPS L1C and L1 C/A code signals. First, the nominal received power of these two signals is discussed along with the power split parameters required for optimal combining. Next, a model for the composite C/A code and L1C signal is presented. The optimal detector for joint acquisition is then derived and simulation results provided. Finally, sub-optimal, but more efficient, techniques are proposed and their performance evaluated by comparing the detection probabilities at a fixed false alarm rate.

## INTRODUCTION

GPS users will have access to two different civil signals at the same frequency within the next several years. The legacy GPS L1 C/A code signal will be joined by the GPS L1C signal with the launch of GPS Block III satellites. L1C is the most recent of the modernized GPS signals and has both a pilot and data component like most other modern GNSS signals. This paper proposes and analyzes various strategies to combine the L1 C/A code and L1C signals for joint acquisition with the goal to improve acquisition performance relative to using either signal alone. Performance is evaluated using the detection and false alarm probabilities. These two signals are transmitted in phase quadrature with the C/A signal lagging L1C by 90 degrees since the L1C signal is transmitted with the same phase as the the L1 P(Y) code military signal.

Acquisition of GNSS signals requires a two-dimensional search for code delay and Doppler frequency of the incoming signal. With the onset of new GNSS signals that have pilot and data components, various joint acquisition schemes have been previously investigated. A simple acquisition scheme can use either component, correlating the received signal with either the pilot or the data spreading code. One obvious disadvantage of this approach is the wasting of signal power; hence, more sophisticated techniques for signal combining or joint acquisition of the pilot and data components have been proposed.

This paper describes methods for improving acquisition sensitivity by using both civil GPS signals on

Table 1: Nominal Received Power Levels

| Signal | Received Power |
|--------|----------------|
| C/A Code | -158.5 dBW |
| L1C Pilot | -158.25 dBW |
| L1C Data | -163 dBW |
| L1C Composite | -157 dBW |

the L1 frequency. Specifically, the strategies previously developed for joint pilot/data acquisition, such as coherent combining [1–5], are extended for joint acquisition of GPS L1 C/A and L1C. In a 2010 paper, Macchi-Gernot, Petovello, and Lachapelle proposed a combined acquisition scheme that uses the FFT to perform parallel code phase search using four different local composite codes which are linear combinations of the C/A, L1C pilot, and L1C data spreading codes to cover all possible relative signs between them [6]. This paper provides detection and false alarm probabilities for this coherent combining scheme.

After first presenting the nominal power levels of the GPS L1 civil signals, a model for the composite C/A and L1C signal is developed. The optimal detector for joint acquisition is then derived and its performance evaluated using Monte Carlo simulations to determine the single trial detection probability at a fixed false alarm rate. Sub-optimal but more efficient joint acquisition techniques are then considered, including non-coherent combining, coherent combining, and semi-coherent combining. Finally, detectors that use the L1C pilot and L1 C/A code, but ignore the lower power L1C data component are presented.

## RECEIVED POWER AND POWER SPLIT PARAMETERS

For optimal detection of composite signals with unequal power levels, the receiver needs to scale each signal by its relative power level. Table 1 shows the nominal received power levels for C/A and L1C according to the specification documents [7,8].

Since the L1C nominal received signal is 1.5 dBW higher than the C/A code, L1C has a received strength that is $10^{\frac{1.5}{10}} = 1.4125$ times higher than C/A on a linear scale:

$$1.4125\gamma + \gamma = 1,$$
$$\gamma = 0.4145, \quad (1)$$

so that C/A has a fraction $\gamma$ of the total power and L1C has a fraction $1 - \gamma$ of the total power in the composite signal. While using the convention that $\alpha$

and $\beta$ represent the power split for the L1C pilot and data components, $\gamma$ is used to represent the power split for the C/A component:

Composite Power =
$$= \alpha(\text{L1C Pilot Power}) + \beta(\text{L1C Data Power})$$
$$+ \gamma(\text{C/A Signal Power})$$
$$= (1-0.4145)\left[\tfrac{3}{4}(\text{L1C Pilot Power})\right.$$
$$\left. + \tfrac{1}{4}(\text{L1C Data Power})\right] + 0.4145(\text{C/A Signal Power})$$
$$= 0.4391(\text{L1C Pilot Power}) + 0.1464(\text{L1C Data Power})$$
$$+ 0.4145(\text{C/A Signal Power}), \quad (2)$$

so that the power split parameters are:

$$\alpha = 0.4391, \ \ \beta = 0.1464 \text{ and } \gamma = 0.4145. \quad (3)$$

These power split parameters are used in both the optimal and sub-optimal detectors for joint acquisition of C/A and L1C. Before proposing the various detectors, a signal model is developed.

## GPS L1C AND SIGNAL MODEL

The design of the new civil signal in the L1 band, called L1C, is described in [9,10]. It has the same carrier frequency of 1575.42 MHz as the legacy L1 C/A code signal but many innovative design features separate this signal from its counterpart on the same frequency that was designed thirty years prior. The signal design for L1C is specified in the Interface Specification document IS-GPS-800A [8].

The L1C signal is split into two components with 75% power in the pilot component and 25% power in the data component. Spreading codes with a length of 10,230 chips and a period of 10 ms at a chipping rate of 1.023 Mcps are based on Weil codes [11]. Not only does each satellite have unique spreading codes, but different codes are also used for the pilot and data components as they are transmitted with the same phase. In addition to the spreading code, the pilot component has an 18 second 1800-bit overlay code. One bit of this overlay code and one bit of the navigation data on the data component both have a duration of 10 ms which corresponds to one period of the spreading code. Both components of the L1C signal use binary offset carrier (BOC) modulation which is explained in [12].

After signal conditioning in the front end of the GNSS receiver, the GPS L1 civil composite signal from one

satellite is

$$
\begin{aligned}
s(t) = {} & \sqrt{2\alpha C}\, d_P(t-\tau) c_P(t-\tau) g_P(t-\tau) \\
& \cdot \cos(2\pi(f_{IF}+f_d)t+\theta) \\
& + \sqrt{2\beta C}\, d_D(t-\tau) c_D(t-\tau) g_D(t-\tau) \\
& \cdot \cos(2\pi(f_{IF}+f_d)t+\theta) \\
& + \sqrt{2\gamma C}\, d_{C/A}(t-\tau) c_{C/A}(t-\tau) \\
& \cdot \sin(2\pi(f_{IF}+f_d)t+\theta) + n(t),
\end{aligned}
\tag{4}
$$

where:

- the total signal power is now denoted as $C$ (Watts), which includes any antenna gain and receiver implementation losses;

- $\alpha$, $\beta$, and $\gamma$ are the power split parameters defined in (3);

- $d_D(t)$, $d_P(t)$, and $d_{C/A}(t)$ are the series of L1C data, L1C overlay code, and C/A data bits;

- $c_D$, $c_P$, and $c_{C/A}$ are the periodic repetition of each spreading code series;

- $g_D(t)$ and $g_P(t)$ are the periodic repetition of the spreading symbols, also called the subcarrier, for the L1C data and pilot components (the C/A code spreading symbol is the rectangular pulse which is fully described by the spreding code);

- $\tau$ and $f_d$ are the unknown delay and Doppler frequency;

- the signal is now at an intermediate frequency $f_{IF}$ (Hertz); and,

- $\theta$ is the unknown phase term.

After multiplication by two reference signals that are in phase quadrature and subsequent low-pass filtering, the inphase and quadrature receiver channels are:

$$
\begin{aligned}
\mathrm{I-Channel} = {} & \sqrt{2\alpha C}\, d_P(t-\tau) c_P(t-\tau) g_P(t-\tau) \\
& \cdot \cos(2\pi\Delta f_d t+\Delta\theta) \\
& + \sqrt{2\beta C}\, d_D(t-\tau) c_D(t-\tau) g_D(t-\tau) \\
& \cdot \cos(2\pi\Delta f_d t+\Delta\theta) \\
& + \sqrt{2\gamma C}\, d_{C/A}(t-\tau) c_{C/A}(t-\tau) \\
& \cdot \sin(2\pi\Delta f_d t+\Delta\theta) + n_I(t),
\end{aligned}
\tag{5}
$$

and

$$
\begin{aligned}
\mathrm{Q-Channel} = {} & \sqrt{2\alpha C}\, d_P(t-\tau) c_P(t-\tau) g_P(t-\tau) \\
& \cdot \sin(2\pi\Delta f_d t+\Delta\theta) \\
& + \sqrt{2\beta C}\, d_D(t-\tau) c_D(t-\tau) g_D(t-\tau) \\
& \cdot \sin(2\pi\Delta f_d t+\Delta\theta) \\
& - \sqrt{2\gamma C}\, d_{C/A}(t-\tau) c_{C/A}(t-\tau) \\
& \cdot \cos(2\pi\Delta f_d t+\Delta\theta) + n_Q(t),
\end{aligned}
\tag{6}
$$

where $\Delta f_d = f_d - \hat{f}_d$ is the error in Doppler estimate, and $\Delta\theta = \theta - \hat{\theta}$ is the carrier phase offset between the local replica and the received signal[1].

The inphase and quadrature channels are coherently-integrated after each is multiplied by the local code, and for L1C, the spreading symbol replicas. Each coherent integration gives a scalar output every integer multiple, $k$, of the coherent integration time, $T_{coh}$:

$$
\begin{aligned}
I_{P,k} ={} & \frac{\sqrt{\alpha C}\, d_{P,k}}{T_{coh}} \int_{kT_{coh}}^{kT_{coh}+T_{coh}} c_P(t-\tau) c_P(t-\hat{\tau}) \\
& \cdot g_P(t-\tau) g_P(t-\hat{\tau}) \cos(2\pi\Delta f_d t+\Delta\theta)\mathrm{d}t + \eta_{P,I,k}, \\
Q_{P,k} ={} & \frac{\sqrt{\alpha C}\, d_{P,k}}{T_{coh}} \int_{kT_{coh}}^{kT_{coh}+T_{coh}} c_P(t-\tau) c_P(t-\hat{\tau}) \\
& \cdot g_P(t-\tau) g_P(t-\hat{\tau}) \sin(2\pi\Delta f_d t+\Delta\theta)\mathrm{d}t + \eta_{P,Q,k}, \\
I_{D,k} ={} & \frac{\sqrt{\beta C}\, d_{D,k}}{T_{coh}} \int_{kT_{coh}}^{kT_{coh}+T_{coh}} c_D(t-\tau) c_D(t-\hat{\tau}) \\
& \cdot g_D(t-\tau) g_D(t-\hat{\tau}) \cos(2\pi\Delta f_d t+\Delta\theta)\mathrm{d}t + \eta_{D,I,k}, \\
Q_{D,k} ={} & \frac{\sqrt{\beta C}\, d_{D,k}}{T_{coh}} \int_{kT_{coh}}^{kT_{coh}+T_{coh}} c_D(t-\tau) c_D(t-\hat{\tau}) \\
& \cdot g_D(t-\tau) g_D(t-\hat{\tau}) \sin(2\pi\Delta f_d t+\Delta\theta)\mathrm{d}t + \eta_{D,Q,k}, \\
I_{C/A,k} ={} & \frac{\sqrt{\gamma C}\, d_{C/A,k}}{T_{cosh}} \int_{kT_{coh}}^{kT_{coh}+T_{coh}} c_{C/A}(t-\tau) \\
& \cdot c_{C/A}(t-\hat{\tau}) \sin(2\pi\Delta f_d t+\Delta\theta)\mathrm{d}t + \eta_{C/A,I,k}, \\
Q_{C/A,k} ={} & \frac{-\sqrt{\gamma C}\, d_{C/A,k}}{T_{coh}} \int_{kT_{coh}}^{kT_{coh}+T_{coh}} c_{C/A}(t-\tau) \\
& \cdot c_{C/A}(t-\hat{\tau}) \cos(2\pi\Delta f_d t+\Delta\theta)\mathrm{d}t + \eta_{C/A,Q,k},
\end{aligned}
\tag{7}
$$

where $\hat{\tau}$ is the estimated delay; and $\eta$ are the uncorrelated noise terms that each have the same variance [13]:

$$
\sigma^2 = N_0/2T_{coh}.
\tag{8}
$$

Two assumptions are applied herein: that the coherent integration time is the length of the L1C spreading code period (10 ms), which is the same as the L1C overlay and data code bit duration; and that bit transitions are avoided. When the signal from the satellite is present, and correct delay ($\hat{\tau}=\tau$) and Doppler estimates are used, the output of the correlators are now:

$$
\begin{aligned}
I_{P,k} &= \sqrt{\alpha C}\, d_{P,k} \cos(\Delta\theta) + \eta_{P,I,k}, \\
Q_{P,k} &= \sqrt{\alpha C}\, d_{P,k} \sin(\Delta\theta) + \eta_{P,Q,k}, \\
I_{D,k} &= \sqrt{\beta C}\, d_{D,k} \cos(\Delta\theta) + \eta_{D,I,k}, \\
Q_{D,k} &= \sqrt{\beta C}\, d_{D,k} \sin(\Delta\theta) + \eta_{D,Q,k}, \\
I_{C/A,k} &= \sqrt{\gamma C}\, d_{C/A,k} \sin(\Delta\theta) + \eta_{C/A,I,k}, \\
Q_{C/A,k} &= -\sqrt{\gamma C}\, d_{C/A,k} \cos(\Delta\theta) + \eta_{C/A,Q,k}.
\end{aligned}
\tag{9}
$$

---

[1]Note that the C/A component in the I-Channel contains the sine term since the C/A code signal lags L1C by 90 degrees, likewise, the C/A component in the Q-Channel contains a negative cosine term.

Due to the autocorrelation properties of the spreading code, the correlator outputs are modeled as noise only when incorrect delay estimates ($\hat{\tau} \neq \tau$) are used. In this joint acquisition scenario however, there are actually incorrect L1C spreading code delay estimates that correspond with correct C/A code phase estimates and will lead to energy in the C/A code correlator outputs, $I_{C/A,k}$ and $Q_{C/A,k}$. The C/A spreading codes repeat every 1ms, while the L1C codes repeat every 10 ms. Noise only for incorrect code phase estimates is still assumed, but these secondary peaks in the correlation due to the repetition of the C/A code within one L1C spreading code period are discussed in the last section. With a model to represent the composite C/A and L1C signal, an optimal detector for acquisition is now investigated.

## OPTIMAL DETECTOR FOR ACQUISITION WITH GPS L1 C/A AND L1C

The optimal detector for joint acquisition of L1 C/A and L1C is derived in the Appendix. This detector provides an upper bound on the performance that can be achieved by combining these two L1 civil signals for GPS acquisition. The likelihood ratio for this optimal detector from (49) is:

$$\Lambda(\mathbf{r}) = \sum_{\mathbf{d}_P, \mathbf{d}_D, \mathbf{d}_{C/A} \in \{B\}} p(\mathbf{d}_P, \mathbf{d}_D, \mathbf{d}_{C/A}) I_0\left(\frac{\sqrt{C}}{\sigma^2}\sqrt{x^2 + y^2}\right), (10)$$

where the vectors $\mathbf{d}$ contain the data during each 10 ms integration for each component, $\{B\}$ is the set of all possible bit combinations, $I_0$ is the modified Bessel function of zeroth order, and $x$ and $y$ are defined as:

$$x = \sum_{k=1}^{K}\left(\sqrt{\alpha}I_{P,k}d_{P,k} + \sqrt{\beta}I_{D,k}d_{D,k} - \sqrt{\gamma}Q_{C/A,k}d_{C/A,k}\right),$$

$$y = \sum_{k=1}^{K}\left(\sqrt{\alpha}Q_{P,k}d_{P,k} + \sqrt{\beta}Q_{D,k}d_{D,k} + \sqrt{\gamma}I_{C/A,k}d_{C/A,k}\right).(11)$$

Unlike the optimal detector for L1C only, presented in [14], the set of all possible bit combinations $\{B\}$ is reduced in this joint case by some impossible combinations of L1C pilot overlay code bits, L1C navigation data bits, and C/A navigation data bits. The bit period for L1C is 10 ms, whereas the bit period for C/A is 20 ms. Since $\mathbf{d}_{C/A}$ represents the navigation bit on C/A every 10 ms, all combinations in which three consecutive C/A data bits are different are not possible and therefore, not included in $\{B\}$. The detection probabilities of the optimal detector for joint acquisition referenced to the C/No of the L1C signal are shown in Figs. 1 and 2, while using one and three spreading code periods.
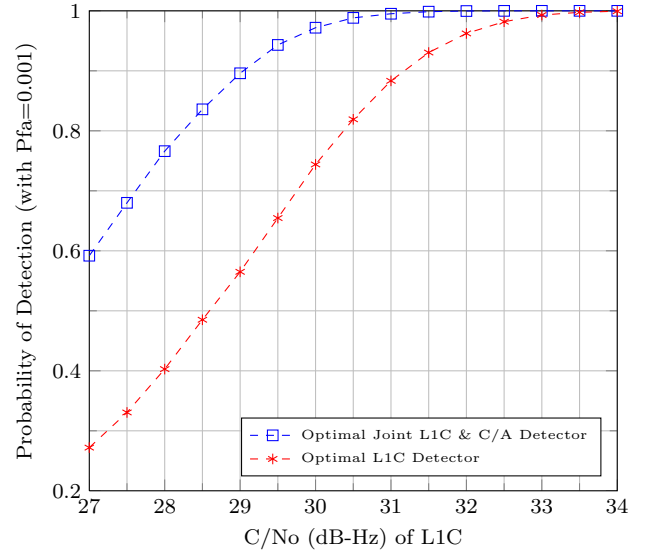


Figure 1: Detection probability of optimal joint L1C and C/A detector compared to optimal L1C detector for acquisition over one L1C spreading code period referenced to L1C signal power.
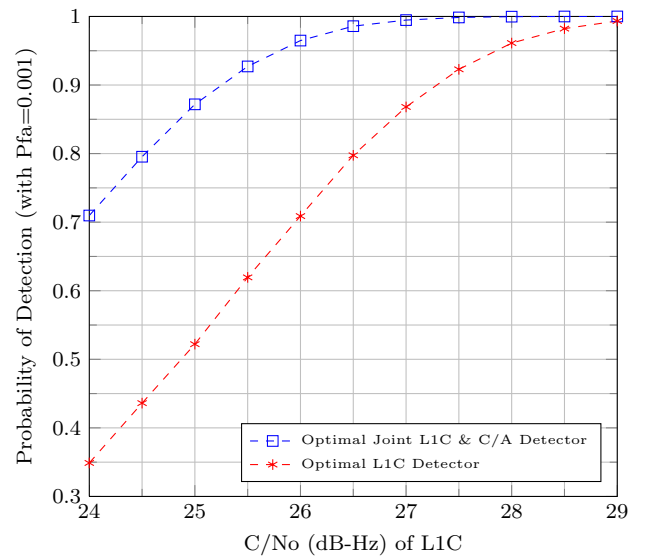


Figure 2: Detection probability of optimal joint L1C and C/A detector compared to optimal L1C detector for acquisition over three L1C spreading code periods referenced to L1C signal power.
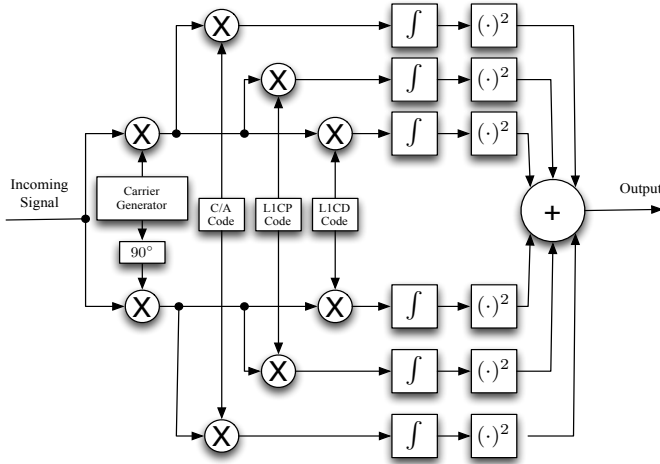
Figure 3: Block diagram of noncoherent combining detector for joint acquisition of GPS L1C and C/A.

## SUB-OPTIMAL DETECTORS FOR JOINT C/A AND L1C ACQUISITION

With the optimal joint detector as a benchmark for the best possible performance of joint acquisition of the legacy C/A code and L1C signals, this section proposes various sub-optimal, but more computationally efficient, detectors.

### Noncoherent Combining

Noncoherent combining is the separate acquisition of each component and the subsequent combination of the correlator powers. The incoming signal can be correlated separately with a local replica of the L1C pilot, the L1C data, and the C/A spreading codes as shown in Fig. 3. Noncoherent channel combining is the squaring, scaling and summing of correlator outputs to obtain the decision variable:

$$Z_{\text{ncw}}^{\text{joint}} = \sum_{k=1}^{K} \Big( \alpha I_{P,k}^2 + \alpha Q_{P,k}^2 + \beta I_{D,k}^2 + \beta Q_{D,k}^2$$
$$+ \gamma I_{C/A,k}^2 + \gamma Q_{C/A,k}^2 \Big), \qquad (12)$$

where $\alpha$, $\beta$, and $\gamma$, are the power split parameters from (3).

Since the underlying Gaussian random variables have three different variances based on the power split factors, the decision statistic, $Z_{\text{ncw}}^{\text{joint}}$, is a sum of three chi-square random variables, each with $2K$ degrees of freedom. When the signal is not present, or when incorrect delay and Doppler estimates are used, the random variables have a central chi-square distribution. When the delay and Doppler estimates are correct, the
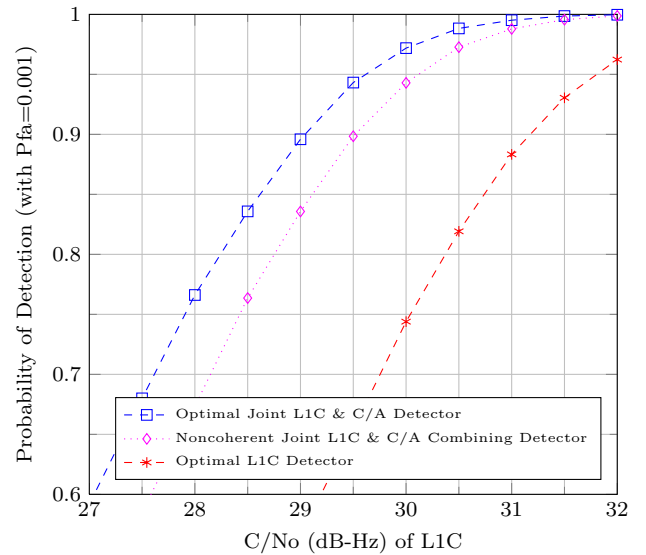


Figure 4: Detection probability of noncoherent combining joint L1C and C/A detector for acquisition over one L1C spreading code period referenced to L1C signal power.

random variables have a non-central chi-square distribution.

Performance results of this noncoherent combining detector using detection probabilities found from Monte Carlo simulations are shown in Figs. 4 and 5. As the total integration time increases, the performance gap between the optimal and noncoherent combining detectors also increases. Other combining techniques to improve performance for joint acquisition are now considered.

### Coherent Combining

If the relative sign between the overlay/data bits on L1C pilot, L1C data, and C/A were known, the three components could be coherently combined [6]. This technique has be studied for acquisition of modern dual component signals [1–5, 15]. In the joint acquisition scheme, the receiver can estimate the relative signs by testing four combinations using the combination with the maximum power as the decision statistic:

$$Z_{\text{chw}}^{\text{joint}} = \max \left\{ |z_1|^2, |z_2|^2, |z_3|^2, |z_4|^2 \right\}, \qquad (13)$$
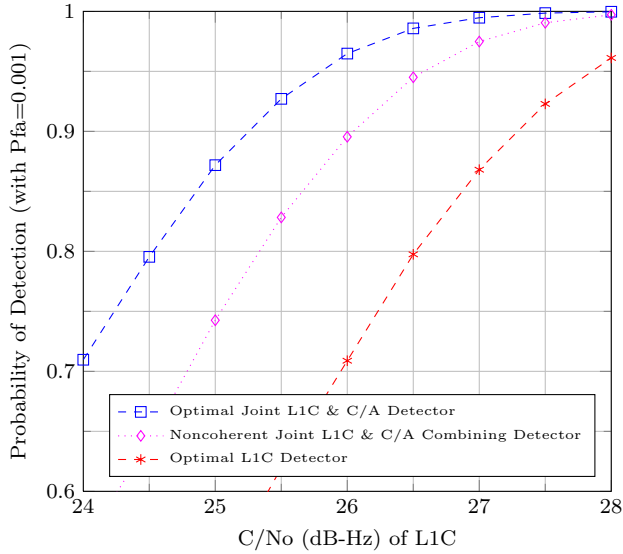
Figure 5: Detection probability of noncoherent combining joint L1C and C/A detector for acquisition over three L1C spreading code periods referenced to L1C signal power.

where:

$$z_1 = \sqrt{\alpha}I_P + j\sqrt{\alpha}Q_P + \sqrt{\beta}I_D + j\sqrt{\beta}Q_D$$
$$- \sqrt{\gamma}Q_{C/A} + j\sqrt{\gamma}I_{C/A}, \quad (14a)$$
$$z_2 = \sqrt{\alpha}I_P + j\sqrt{\alpha}Q_P + \sqrt{\beta}I_D + j\sqrt{\beta}Q_D$$
$$+ \sqrt{\gamma}Q_{C/A} - j\sqrt{\gamma}I_{C/A}, \quad (14b)$$
$$z_3 = \sqrt{\alpha}I_P + j\sqrt{\alpha}Q_P - \sqrt{\beta}I_D - j\sqrt{\beta}Q_D$$
$$+ \sqrt{\gamma}Q_{C/A} - j\sqrt{\gamma}I_{C/A}, \quad (14c)$$
$$z_4 = \sqrt{\alpha}I_P + j\sqrt{\alpha}Q_P - \sqrt{\beta}I_D - j\sqrt{\beta}Q_D$$
$$- \sqrt{\gamma}Q_{C/A} + j\sqrt{\gamma}I_{C/A}, \quad (14d)$$

and

$$|z_1|^2 = \left(\sqrt{\alpha}I_P + \sqrt{\beta}I_D - \sqrt{\gamma}Q_{C/A}\right)^2$$
$$+ \left(\sqrt{\alpha}Q_P + \sqrt{\beta}Q_D + \sqrt{\gamma}I_{C/A}\right)^2, \quad (15a)$$
$$|z_2|^2 = \left(\sqrt{\alpha}I_P + \sqrt{\beta}I_D + \sqrt{\gamma}Q_{C/A}\right)^2$$
$$+ \left(\sqrt{\alpha}Q_P + \sqrt{\beta}Q_D - \sqrt{\gamma}I_{C/A}\right)^2, \quad (15b)$$
$$|z_3|^2 = \left(\sqrt{\alpha}I_P - \sqrt{\beta}I_D + \sqrt{\gamma}Q_{C/A}\right)^2$$
$$+ \left(\sqrt{\alpha}Q_P - \sqrt{\beta}Q_D - \sqrt{\gamma}I_{C/A}\right)^2, \quad (15c)$$
$$|z_4|^2 = \left(\sqrt{\alpha}I_P - \sqrt{\beta}I_D - \sqrt{\gamma}Q_{C/A}\right)^2$$
$$+ \left(\sqrt{\alpha}Q_P - \sqrt{\beta}Q_D + \sqrt{\gamma}I_{C/A}\right)^2, \quad (15d)$$

with:

$$\alpha = 0.4391, \ \beta = 0.1464 \text{ and } \gamma = 0.4145.$$

The powers of the various combinations, $|z_x|^2$, are chi-square random variables with two degrees of freedom. With the weights applied for the unequal power compensation, the underlying Gaussian random variables have a variance of $\sigma^2$. Without the unequal power compensation, the variance of the underlying Gaussian random variables in the chi-square random variable would be $3\sigma^2$. When the desired signal is not present or with incorrect code delay and Doppler estimates, the $|z_x|^2$ terms are central chi-square random variables.

When the signal is present with correct estimates of delay and Doppler, their are four possibilities for the non-centrality parameter, depending on the relative sign between the overlay/data bits on the three components. For $|z_1|^2$, the noncentrality parameter is:

$$a_1^2 = \left(\alpha\sqrt{C}d_P\cos(\Delta\theta) + \beta\sqrt{C}d_D\cos(\Delta\theta)\right.$$
$$\left. + \gamma\sqrt{C}d_{C/A}\cos(\Delta\theta)\right)^2$$
$$+ \left(\alpha\sqrt{C}d_P\sin(\Delta\theta) + \beta\sqrt{C}d_D\sin(\Delta\theta)\right.$$
$$\left. + \gamma\sqrt{C}d_{C/A}\sin(\Delta\theta)\right)^2$$
$$= \begin{cases} (\alpha+\beta+\gamma)^2 C = C, \text{ correct rel. signs,} \\ (\alpha^2+\beta^2+\gamma^2+2\alpha\beta-2\alpha\gamma-2\beta\gamma) C, \text{ or} \\ (\alpha^2+\beta^2+\gamma^2-2\alpha\beta-2\alpha\gamma+2\beta\gamma) C, \text{ or} \\ (\alpha^2+\beta^2+\gamma^2-2\alpha\beta+2\alpha\gamma-2\beta\gamma) C. \end{cases} \quad (16)$$

Using the values for $\alpha$, $\beta$, and $\gamma$, the noncentrality parameter is:

$$a_1^2 = \begin{cases} C, \left(d_Pd_{C/A} = d_Pd_{C/A} = +1\right) \\ 0.0292C, \ \left(d_Pd_{C/A} = d_Pd_{C/A} = -1\right) \\ 0.0148C, \ \left(d_Pd_{C/A} = -1, d_Pd_{C/A} = +1\right) \\ 0.5001C, \ \left(d_Pd_{C/A} = +1, d_Pd_{C/A} = -1\right). \end{cases} \quad (17)$$

Likewise, the noncentrality parameters for the other three combinations are:

$$a_2^2 = \begin{cases} 0.0292C, \left(d_Pd_{C/A} = d_Pd_{C/A} = +1\right) \\ C, \left(d_Pd_{C/A} = d_Pd_{C/A} = -1\right) \\ 0.5001C, \left(d_Pd_{C/A} = -1, d_Pd_{C/A} = +1\right) \\ 0.0148C, \left(d_Pd_{C/A} = +1, d_Pd_{C/A} = -1\right), \end{cases} \quad (18)$$

and

$$a_3^2 = \begin{cases} 0.0148C, \left(d_Pd_{C/A} = d_Pd_{C/A} = +1\right) \\ 0.5001C, \left(d_Pd_{C/A} = d_Pd_{C/A} = -1\right) \\ C, \left(d_Pd_{C/A} = -1, d_Pd_{C/A} = +1\right) \\ 0.0292C, \left(d_Pd_{C/A} = +1, d_Pd_{C/A} = -1\right), \end{cases} \quad (19)$$

and

$$a_4^2 = \begin{cases} 0.5001C, & \left(d_P d_{C/A} = d_P d_{C/A} = +1\right) \\ 0.0148C, & \left(d_P d_{C/A} = d_P d_{C/A} = -1\right) \\ 0.0292C, & \left(d_P d_{C/A} = -1, d_P d_{C/A} = +1\right) \\ C, & \left(d_P d_{C/A} = +1, d_P d_{C/A} = -1\right). \end{cases} \quad (20)$$

Using the fact motivated by [5] that

$$\begin{aligned} P(Z > \lambda) &= P\left(\max\left\{|z_1|^2, |z_2|^2, |z_3|^2, |z_4|^2\right\} > \lambda\right) \\ &= 1 - P\left(\max\left\{|z_1|^2, |z_2|^2, |z_3|^2, |z_4|^2\right\} < \lambda\right) \\ &= 1 - P\left(|z_1|^2 < \lambda, |z_2|^2 < \lambda, |z_3|^2 < \lambda, |z_4|^2 < \lambda\right) \\ &= 1 - P\left(|z_1|^2 < \lambda\right) P\left(|z_2|^2 < \lambda\right) \\ &\quad \cdot P\left(|z_3|^2 < \lambda\right) P\left(|z_4|^2 < \lambda\right), \end{aligned} \quad (21)$$

the noncentrality parameters lead to the following false alarm and detection probabilities for joint acquisition using coherent combining:

$$\begin{aligned} P_{fa}^{joint,chw}(\lambda) &= 1 - P\left(|z_1|^2 < \lambda \mid H_0\right) P\left(|z_2|^2 < \lambda \mid H_0\right) \\ &\quad P\left(|z_3|^2 < \lambda \mid H_0\right) P\left(|z_4|^2 < \lambda \mid H_0\right) \\ &= 1 - \left[1 - \exp\left(\frac{-\lambda}{2\sigma^2}\right)\right]^4, \end{aligned} \quad (22)$$

and

$$\begin{aligned} P_d^{joint,chw}&(\lambda) \\ &= 1 - P\left(|z_1|^2 < \lambda \mid H_1\right) P\left(|z_2|^2 < \lambda \mid H_1\right) \\ &\quad P\left(|z_3|^2 < \lambda \mid H_1\right) P\left(|z_4|^2 < \lambda \mid H_1\right) \\ &= 1 - \left[1 - Q_1\left(\frac{\sqrt{C}}{\sigma}, \frac{\sqrt{\lambda}}{\sigma}\right)\right]\left[1 - Q_1\left(\frac{\sqrt{0.0292C}}{\sigma}, \frac{\sqrt{\lambda}}{\sigma}\right)\right] \\ &\quad \cdot \left[1 - Q_1\left(\frac{\sqrt{0.0148C}}{\sigma}, \frac{\sqrt{\lambda}}{\sigma}\right)\right]\left[1 - Q_1\left(\frac{\sqrt{0.5001C}}{\sigma}, \frac{\sqrt{\lambda}}{\sigma}\right)\right], \end{aligned}$$

where $Q_1$ is the Marcum's Q function. Fig. 6 shows that this coherent combining technique for joint acquisition of all GPS L1 civil signals has similar performance to the optimal detector. This technique can be extended over multiple L1C spreading code periods by using semi-coherent integration.

**Semi-Coherent Integration**

The coherent combinations of GPS L1C pilot, L1C data, and C/A code every 10 ms coherent integration period can be noncoherently combined using an integer number $K$ sequential coherent combinations in a technique known as semi-coherent integration:

$$Z_{\text{semi}}^{\text{joint}} = \sum_{k=1}^{K} \max\left\{|z_{1,k}|^2, |z_{2,k}|^2, |z_{3,k}|^2, |z_{4,k}|^2\right\}, \quad (23)$$
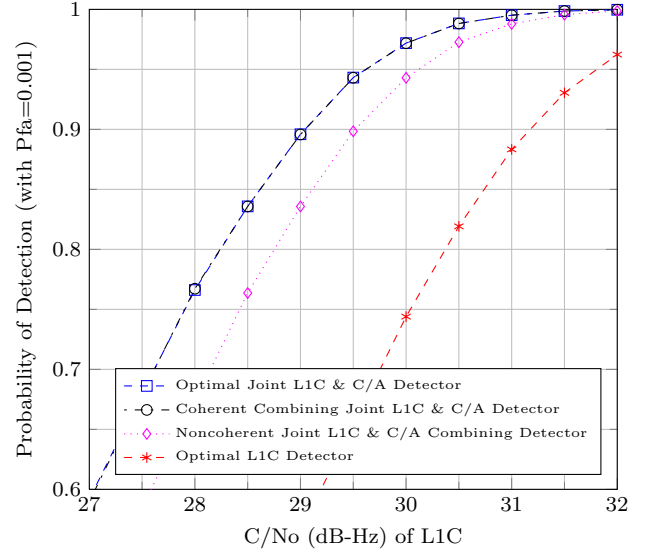


Figure 6: Detection probability of coherent combining joint L1C and C/A detector for acquisition over one L1C spreading code period referenced to L1C signal power.

where:

$$\begin{aligned} |z_{1,k}|^2 &= \left(\sqrt{\alpha}I_{P,k} + \sqrt{\beta}I_{D,k} - \sqrt{\gamma}Q_{C/A,k}\right)^2 \\ &\quad + \left(\sqrt{\alpha}Q_{P,k} + \sqrt{\beta}Q_{D,k} + \sqrt{\gamma}I_{C/A,k}\right)^2 \quad (24\text{a}) \end{aligned}$$

$$\begin{aligned} |z_{2,k}|^2 &= \left(\sqrt{\alpha}I_{P,k} + \sqrt{\beta}I_{D,k} + \sqrt{\gamma}Q_{C/A,k}\right)^2 \\ &\quad + \left(\sqrt{\alpha}Q_{P,k} + \sqrt{\beta}Q_{D,k} - \sqrt{\gamma}I_{C/A,k}\right)^2 \quad (24\text{b}) \end{aligned}$$

$$\begin{aligned} |z_{3,k}|^2 &= \left(\sqrt{\alpha}I_{P,k} - \sqrt{\beta}I_{D,k} + \sqrt{\gamma}Q_{C/A,k}\right)^2 \\ &\quad + \left(\sqrt{\alpha}Q_{P,k} - \sqrt{\beta}Q_{D,k} - \sqrt{\gamma}I_{C/A,k}\right)^2 \quad (24\text{c}) \end{aligned}$$

$$\begin{aligned} |z_{4,k}|^2 &= \left(\sqrt{\alpha}I_{P,k} - \sqrt{\beta}I_{D,k} - \sqrt{\gamma}Q_{C/A,k}\right)^2 \\ &\quad + \left(\sqrt{\alpha}Q_{P,k} - \sqrt{\beta}Q_{D,k} + \sqrt{\gamma}I_{C/A,k}\right)^2. \quad (24\text{d}) \end{aligned}$$

Simulation results are used in Fig. 7 to show how this semi-coherent integration technique outperforms the noncoherent detector for acquisition over three L1C spreading code periods (30 ms).

Since the coherent combinations depend on relative sign estimates between the overlay/data bits, the performance advantage of semi-coherent integration over noncoherent combining is expected to disappear eventually as the C/No decreases. Fig. 8 shows this point with an extended integration time.
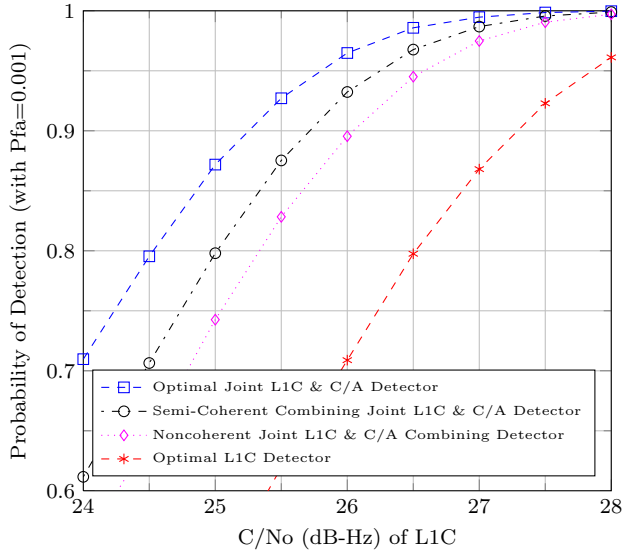
Figure 7: Detection probability of semi-coherent joint L1C and C/A detector for acquisition over three L1C spreading code periods referenced to L1C signal power.
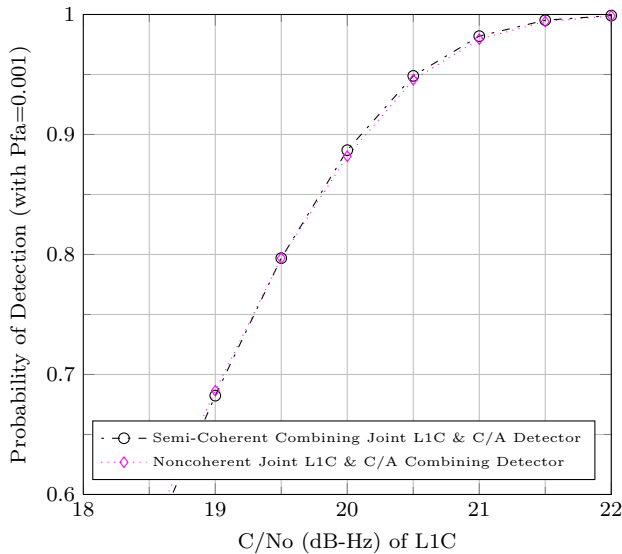


Figure 8: Detection probability of semi-coherent joint L1C and C/A detector for acquisition with an extended integration time over twenty-five spreading code periods referenced to L1C signal power.

## JOINT L1C PILOT AND L1 C/A ACQUISITION

Joint acquisition of the GPS L1C and C/A code signals is an attractive solution to improving acquisition sensitivity. The cost, however, is increased receiver complexity and additional correlator requirements. In the composite L1C and L1 C/A code signal, the L1C data component contributes less than 15 percent of the total signal power. One possible tradeoff is to ignore the L1C data component and perform joint L1C pilot and C/A code acquisition. In this section, detectors that use only the pilot component of L1C along with the C/A code signal for acquisition are proposed and their performance is analyzed.

### Optimal

Since the L1C pilot nominal received signal is 0.25 dBW higher than the C/A code, L1C pilot has a received strength that is $10^{\frac{0.25}{10}} = 1.0593$ times higher than C/A on a linear scale:

$$1.0593\gamma' + \gamma' = 1,$$
$$\gamma' = 0.4856, \qquad (25)$$

so that the power split parameters are:

$$\alpha' = 0.5144, \text{ and } \gamma' = 0.4856. \qquad (26)$$

The likelihood ratio in the optimal detector for joint acquisition of L1C pilot and L1 C/A comes directly from making adjustments to the optimal joint detector in (11) which results in:

$$\Lambda(\mathbf{r}) = \sum_{\mathbf{d}_P, \mathbf{d}_{C/A} \in \{B\}} p(\mathbf{d}_P, \mathbf{d}_{C/A}) I_0 \left( \frac{\sqrt{C'}}{\sigma^2} \sqrt{x^2 + y^2} \right), \quad (27)$$

where $C'$ represents the total received signal power from the two components, the vectors $\mathbf{d}$ contain the overlay/data bits during each 10 ms integration for each component, $\{B\}$ is the set of all possible bit combinations, $I_0$ is the modified Bessel function of zeroth order, and $x$ and $y$ are defined as:

$$x = \sum_{k=1}^{K} \left( \sqrt{\alpha'} I_{P,k} d_{P,k} - \sqrt{\gamma'} Q_{C/A,k} d_{C/A,k} \right),$$
$$y = \sum_{k=1}^{K} \left( \sqrt{\alpha'} Q_{P,k} d_{P,k} + \sqrt{\gamma'} I_{C/A,k} d_{C/A,k} \right). \quad (28)$$

The detection probabilities of this optimal detector for joint L1C pilot and L1 C/A acquisition referenced to the C/No of the L1C signal are shown in Figs. 9 and 10, while using one and three spreading code periods.
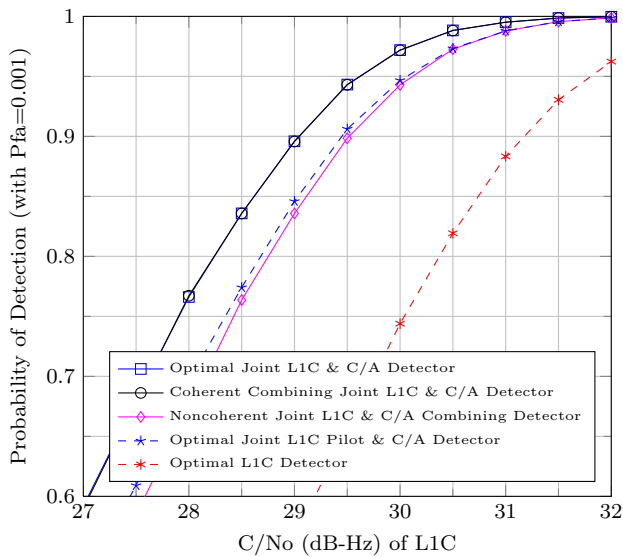
Figure 9: Detection probability of optimal joint L1C pilot and C/A detector for acquisition over one L1C spreading code period referenced to L1C signal power.

The C/No is still referenced to the L1C signals so that the performance of the joint L1C pilot and C/A code detectors can easily be compared to previous acquisition schemes.

**Noncoherent Combining**

Noncoherent combining is the separate acquisition of the L1C pilot component and the C/A code, and the subsequent combination of their correlator powers. The incoming signal can be correlated separately with a local replica of the L1C pilot and the C/A spreading codes as shown in Fig. 11. Noncoherent channel combining is the squaring, scaling and summing of correlator outputs to obtain the decision variable:

$$Z_{\text{ncw}}^{\text{jointpc}} = \sum_{k=1}^{K} \left( \alpha' I_{P,k}^2 + \alpha' Q_{P,k}^2 + \gamma' I_{C/A,k}^2 + \gamma' Q_{C/A,k}^2 \right), (29)$$

where $\alpha'$, and $\gamma'$, are the power split parameters from (26).

Since the underlying Gaussian random variables have two different variances based on the power split factors, the decision statistic, $Z_{\text{ncw}}^{\text{jointpc}}$, is a sum of two chi-square random variables, each with $2K$ degrees of freedom. When the signal is not present, or when incorrect delay and Doppler estimates are used, the random variables have a central chi-square distribution. When the delay and Doppler estimates are correct, the random variables have a non-central chi-square distribution.
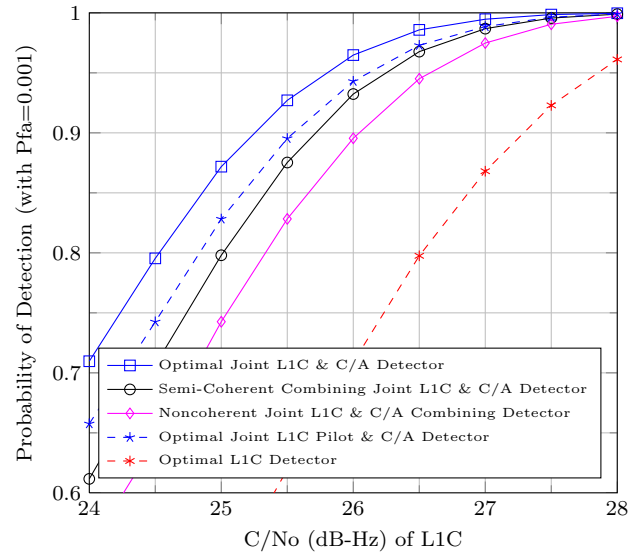


Figure 10: Detection probability of optimal joint L1C pilot and C/A detector for acquisition over three L1C spreading code periods referenced to L1C signal power.
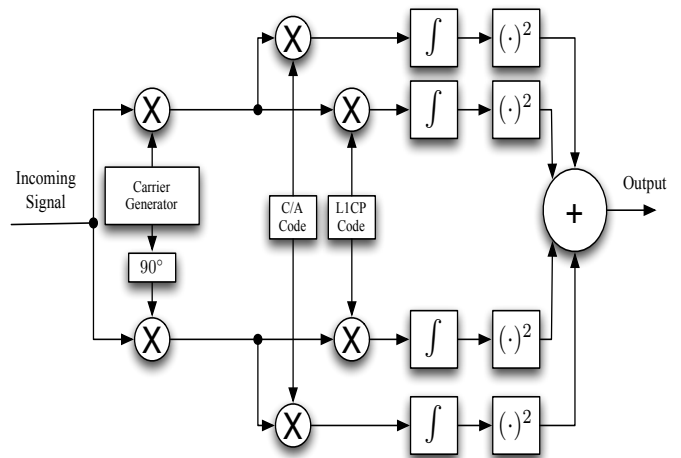


Figure 11: Block diagram of noncoherent combining detector for joint acquisition of GPS L1C Pilot and L1 C/A.
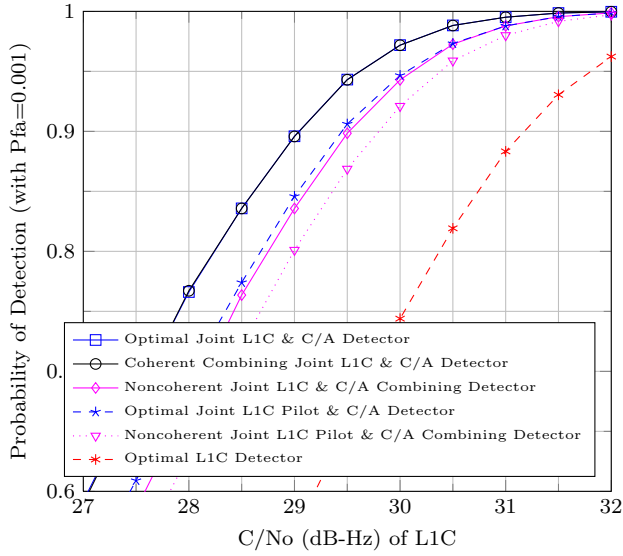
Figure 12: Detection probability of noncoherent combining joint L1C pilot and C/A detector for acquisition over one L1C spreading code period referenced to L1C signal power.



Figure 13: Detection probability of noncoherent combining joint L1C pilot and C/A detector for acquisition over three L1C spreading code periods referenced to L1C signal power.

Performance of this noncoherent combining detector is shown in Figs. 12 and 13. As the total integration time increases, the performance gap between the optimal and noncoherent combining detectors also increases. Other combining techniques to improve performance for joint acquisition of the L1C pilot and C/A code are now considered.

**Coherent Combining**

The coherent channel combining technique presented for the the two L1C components in [15] is adjusted so that the L1C data component is replaced by the C/A code:

$$Z_{\text{chw}}^{\text{jointpc}} = \max\left\{|z^+|^2, |z^-|^2\right\}, \quad (30)$$

where:

$$z^+ = \sqrt{\alpha'}I_P + j\sqrt{\alpha'}Q_P - \sqrt{\gamma'}Q_{C/A} + j\sqrt{\gamma'}I_{C/A}, \quad (31a)$$
$$z^- = \sqrt{\alpha'}I_P + j\sqrt{\alpha'}Q_P + \sqrt{\gamma'}Q_{C/A} - j\sqrt{\gamma'}I_{C/A}, \quad (31b)$$

and

$$|z^+|^2 = \left(\sqrt{\alpha'}I_P - \sqrt{\gamma'}Q_{C/A}\right)^2 + \left(\sqrt{\alpha'}Q_P + \sqrt{\gamma'}I_{C/A}\right)^2 \quad (32a)$$
$$|z^-|^2 = \left(\sqrt{\alpha'}I_P + \sqrt{\gamma'}Q_{C/A}\right)^2 + \left(\sqrt{\alpha'}Q_P - \sqrt{\gamma'}I_{C/A}\right)^2 \quad (32b)$$

The $|z^+|^2$ and $|z^-|^2$ terms are chi-square random variables with two degrees of freedom. With the scale factors, the underlying Gaussian random variables have a varian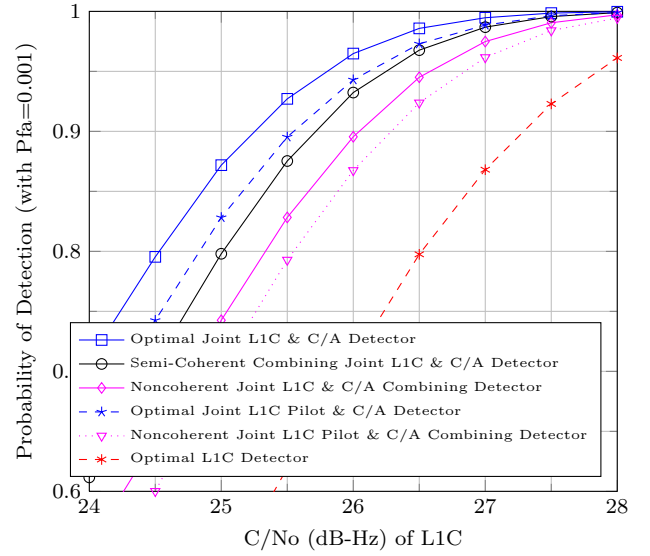ce of $\sigma^2$, instead of $2\sigma^2$. When the signal is present with correct estimates of delay and Doppler, the noncentrality parameter for $|z^+|^2$ is:

$$
\begin{aligned}
a_+^2 &= \left(\alpha'\sqrt{C'}d_P\cos(\Delta\theta) + \gamma'\sqrt{C'}d_{C/A}\cos(\Delta\theta)\right)^2 \\
&\quad + \left(\alpha'\sqrt{C'}d_P\sin(\Delta\theta) + \gamma'\sqrt{C'}d_{C/A}\sin(\Delta\theta)\right)^2 \\
&= \left(\alpha'^2 + \gamma'^2 + 2\alpha'\gamma'd_Pd_{C/A}\right)C\cos^2(\Delta\theta) \\
&\quad + \left(\alpha'^2 + \gamma'^2 + 2\alpha'\gamma'd_Pd_{C/A}\right)C\sin^2(\Delta\theta) \\
&= \left(\alpha'^2 + \gamma'^2 + 2\alpha'\gamma'd_Pd_{C/A}\right)C \\
&= \begin{cases} C, & \left(d_Pd_{C/A} = +1\right) \\ (0.0008)C, & \left(d_Pd_{C/A} = -1\right). \end{cases}
\end{aligned}
\quad (33)
$$

The noncentrality parameter for $|z^-|^2$ is:

$$
\begin{aligned}
a_-^2 &= \left(\alpha'^2 + \gamma'^2 - 2\alpha'\gamma'd_Pd_{C/A}\right)C \\
&= \begin{cases} C, & \left(d_Pd_{C/A} = -1\right) \\ (0.0008)C, & \left(d_Pd_{C/A} = +1\right). \end{cases}
\end{aligned}
\quad (34)
$$

These noncentrality parameters lead to the following false alarm and detection probabilities:

$$
\begin{aligned}
P_{fa}^{chw}(\lambda) &= 1 - P\left(|z^+|^2 < \lambda \mid H_0\right)P\left(|z^-|^2 < \lambda \mid H_0\right) \\
&= 1 - \left[1 - \exp\left(\frac{-\lambda}{2\sigma^2}\right)\right]^2,
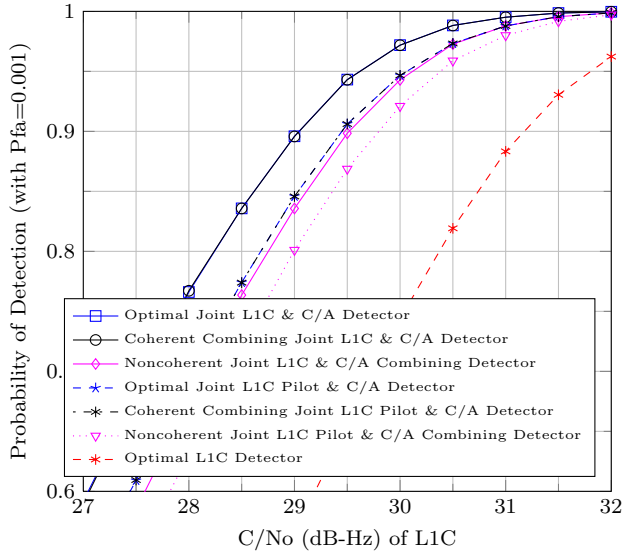\end{aligned}
\quad (35)
$$

Figure 14: Detection probability of coherent combining joint L1C pilot and C/A detector for acquisition over one L1C spreading code period referenced to L1C signal power.
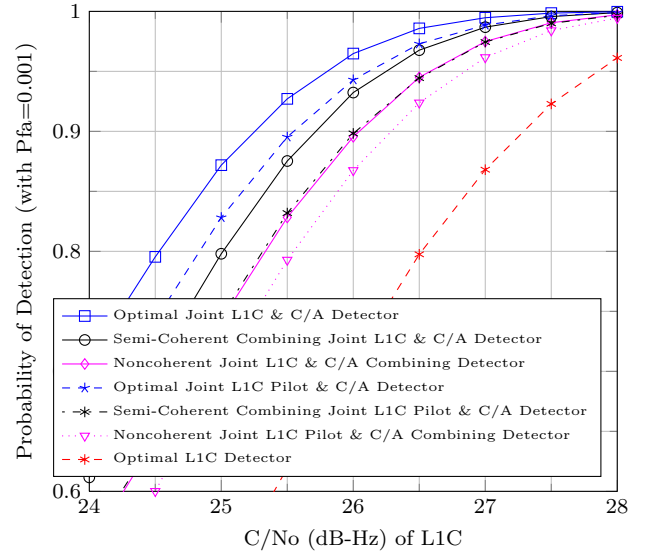


Figure 15: Detection probability of semi-coherent combining joint L1C pilot and C/A detector for acquisition over three L1C spreading code periods referenced to L1C signal power.

and

$$P_d^{chw}(\lambda) = 1 - P\left(|z^+|^2 < \lambda \mid H_1\right) P\left(|z^-|^2 < \lambda \mid H_1\right)$$
$$= 1 - \left[1 - Q_1\left(\frac{\sqrt{C}}{\sigma}, \frac{\sqrt{\lambda}}{\sigma}\right)\right]$$
$$\cdot \left[1 - Q_1\left(\frac{\sqrt{(0.0008)C}}{\sigma}, \frac{\sqrt{\lambda}}{\sigma}\right)\right], \quad (36)$$

where $Q_1$ is the Marcum's Q function. Fig. 14 shows that this coherent combining technique for joint acquisition of all GPS L1 civil signals has similar performance to the optimal detector. This technique can be extended over multiple L1C spreading code periods by using semi-coherent integration.

**Semi-Coherent Integration**

Extending the total integration time by noncoherently combining the 10 ms coherent combinations from the previous section is known as semi-coherent integration:

$$Z_{\text{chw}}^{\text{jointpc}} = \sum_{k=1}^{K} \max\left\{|z_k^+|^2, |z_k^-|^2\right\}, \quad (37)$$

where:

$$|z_k^+|^2 = \left(\sqrt{\alpha'}I_{P,k} - \sqrt{\gamma'}Q_{C/A,k}\right)^2$$
$$+ \left(\sqrt{\alpha'}Q_{P,k} + \sqrt{\gamma'}I_{C/A,k}\right)^2, \quad (38a)$$
$$|z_k^-|^2 = \left(\sqrt{\alpha'}I_{P,k} + \sqrt{\gamma'}Q_{C/A,k}\right)^2$$
$$+ \left(\sqrt{\alpha'}Q_{P,k} - \sqrt{\gamma'}I_{C/A,k}\right)^2. \quad (38b)$$

Simulation results are used in Fig. 15 to show how this semi-coherent integration technique outperforms the noncoherent detector for acquisition over three L1C spreading code periods (30 ms). Since the coherent combinations depend on relative sign estimates between the overlay/data bits, the performance advantage of semi-coherent integration over noncoherent combining is expected to disappear eventually as the C/No decreases. Fig. 16 shows this point with an extended integration time of twenty-five spreading code periods.

**CORRECT C/A CODE PHASE AND INCORRECT L1C CODE PHASE**

The previous work in this paper is based on the assumption that when incorrect estimates for code delay and Doppler are used, the outputs of the correlators contain the noise terms only. The scenario when this assumption is invalid is discussed in this section. The coherent integration time in the acquisition schemes
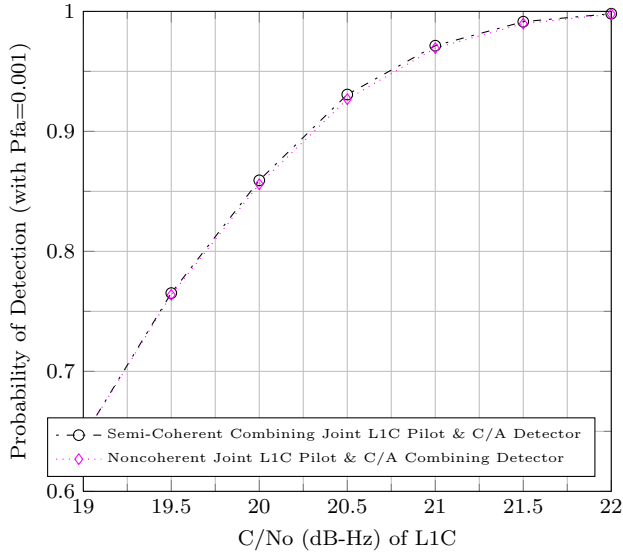
Figure 16: Detection probability of semi-coherent combining joint L1C pilot and C/A detector for acquisition over extended integration time of twenty-five spreading code period referenced to L1C signal power.
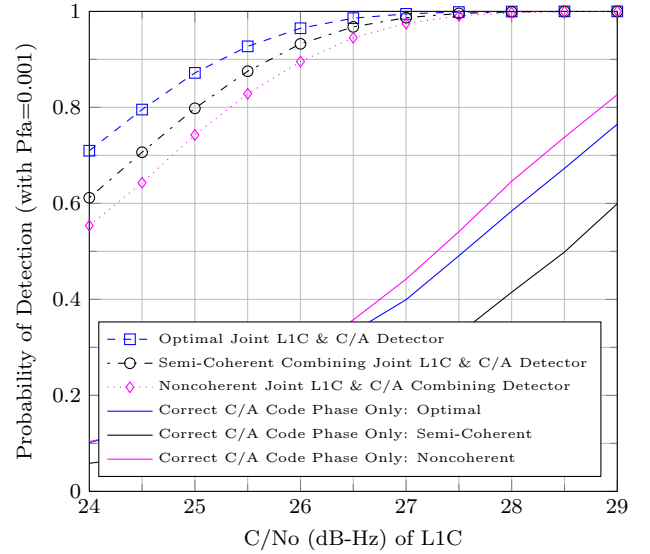


Figure 17: Detection probability of joint L1C and C/A detectors with incorrect L1C code phase estimate but correct C/A code phase estimate for acquisition over three L1C spreading code periods referenced to L1C signal power.

presented here is the length of the L1C spreading code, or 10 ms. Since the L1 C/A code period is only 1ms, it repeats ten times during one L1C spreading code period. This leads to the situation that nine different code delay estimates will be incorrect for L1C but correct for L1 C/A. If correlator spacing of one chip is used, then nine out of 10,230 possible code phase estimates will have noise only on the L1C correlator outputs while having signal energy in the C/A code correlator outputs:

$$
\begin{aligned}
I_{P,k} &= \eta_{P,I,k}, \\
Q_{P,k} &= \eta_{P,Q,k}, \\
I_{D,k} &= \eta_{D,I,k}, \\
Q_{D,k} &= \eta_{D,Q,k}, \\
I_{C/A,k} &= \sqrt{\gamma C}\, d_{C/A,k} \sin\left(\Delta\theta\right) + \eta_{C/A,I,k}, \\
Q_{C/A,k} &= -\sqrt{\gamma C}\, d_{C/A,k} \cos\left(\Delta\theta\right) + \eta_{C/A,Q,k}. \quad (39)
\end{aligned}
$$

A strategy to deal with this possibility may be implemented in the GPS receiver. For example, if the decision statistic of a particular detector crosses the detection threshold, power in the L1C correlator outputs can be checked. If it determined that the correct C/A code phase but incorrect L1C code phase has been found, acquisition can proceed with just the C/A code signal.

To determine the probability that an incorrect L1C code delay estimate but correct C/A code delay estimate would cross the detection threshold, Monte Carlo

simulations with this scenario were performed for the various joint detection schemes presented in this paper. Figs. 17 and 18 show the detection probability various detectors along with the detection probability for a correct C/A code phase but incorrect L1C code phase for each detector. The latter can almost be considered a C/A code detector, however, the detector does contain extra noise terms from the L1C correlators.

## CONCLUSIONS

The trend for future GNSS receivers is multi-signal and multi-constellation capability. Receiver manufacturers are seeking to design devices that use multiple signals from a system while also using multiple satellite navigation systems to get a position, navigation, and timing solution. This paper aids this trend by focusing on joint detection schemes for acquisition of the composite L1C and L1 C/A signal in order to improve acquisition sensitivity.

The optimal detector for joint GPS L1C and L1 C/A was derived and its performance used as a benchmark for other joint acquisition schemes. Coherent combining over one L1C spreading code period by trying all four possible coherent combinations was shown to have optimal performance over one L1C spreading code period. Analytical expressions for the detection and false alarm probabilities were derived. Semi-coherent inte-
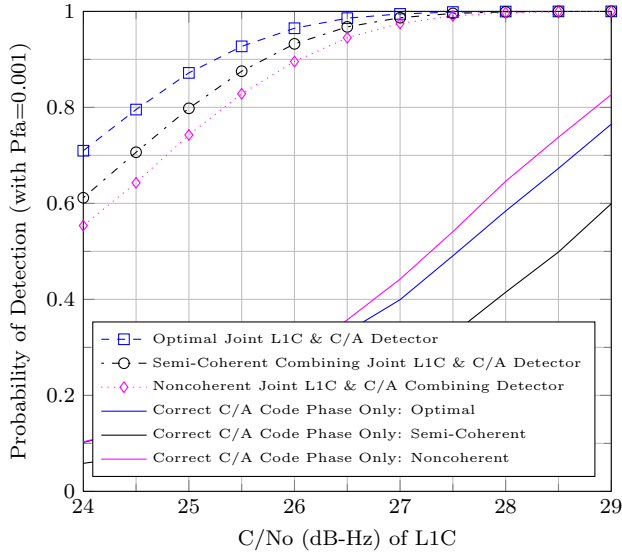
Figure 18: Detection probability of joint L1C pilot and C/A detectors with incorrect L1C code phase estimate but correct C/A code phase estimate for acquisition over three L1C spreading code periods referenced to L1C signal power.

gration used these coherent combinations over multiple spreading code periods. Similar techniques for acquisition were also considered for only using the L1C pilot component along with the C/A code signal. This latter technique may be most attractive to GNSS receiver designers due to the low power contribution from the L1C data component.

## APPENDIX: DERIVATION OF THE OPTIMAL DETECTOR FOR JOINT L1C AND C/A ACQUISITION

In this appendix, classical detection theory is used, following the same procedure used in for L1C only in [14], to derive the optimal detector for joint L1C and C/A acquisition. Processing is performed over an arbitrary integer number of primary spreading code periods of the GPS L1C signal. The signal specification requires that the spreading code chips for the two signals be synchronized [8]; therefore, each period of the L1C code is assumed to contain 10 complete periods of the C/A code. Despite having a shorter spreading code period, C/A code has a data bit duration that is twice as long as L1C: $T_{d,C/A} = 20$ ms. Possible data transitions on the C/A signal occur at the same time as every other possible data transition on each L1C component.

The outputs of the correlators are used here as the observation since they are sufficient statistics for de-

tecting the signal in an additive white Gaussian noise channel [16, 17]. Due to autocorrelation properties of the codes, it is assumed that the correlator outputs contain noise only if an incorrect delay estimate is used. If the correlation outputs are observed every 10 ms a total of K times, then observation at the output of the complex correlators are the following two hypotheses:

$$H_1: \mathbf{r} = \begin{bmatrix} \sqrt{\alpha C}\mathbf{d}_P e^{j\Delta\theta} \\ \sqrt{\beta C}\mathbf{d}_D e^{j\Delta\theta} \\ \sqrt{\gamma C}\mathbf{d}_{C/A}\left(-je^{j\Delta\theta}\right) \end{bmatrix} + \mathbf{n}$$

$$H_0: \mathbf{r} = \mathbf{n}, \tag{40}$$

where the data, $\mathbf{d}_P$, $\mathbf{d}_D$ and $\mathbf{d}_{C/A}$, are each $K \times 1$ vectors which contain the data bit during 10 ms correlation. Under $H_1$, the observation is the $3K \times 1$ vector of correlator outputs from the $K \times 10$ ms observation. The $3K \times 1$ noise vector, $\mathbf{n}$, is white and Gaussian with covariance $\sigma^2\mathbf{I}$, where $\mathbf{I}$ is the identity matrix and $\sigma^2 = N_0/(2T_c)$ [13]. The received signal power is $C$, with the parameters $\alpha$, $\beta$ and $\gamma$ describing the power split among the three components (L1C Pilot, L1C Data, C/A Code), so that $\alpha + \beta + \gamma = 1$. For the joint GPS L1C and C/A acquisition, $\alpha = 20/48$, $\beta = 7/48$ and $\gamma = 20/48$ as noted in (3). The carrier phase residual is $\Delta\theta$. Each component contains data which represent any navigation bits, overlay code, or a combination of these two items which may be present.

Since the *a priori* probabilities of a signal's presence are unknown, the Neyman-Pearson criterion is used to maximize the probability of detection ($P_d$) under a particular probability of false alarm constraint ($P_f$). The optimum test consists of using the observation $\mathbf{r}$ to find the likelihood ratio $\Lambda(\mathbf{r})$ and comparing this result to a threshold to make a decision [16]. The likelihood ratio consists of conditional joint probabilities:

$$\Lambda(\mathbf{r}) \triangleq \frac{p(\mathbf{r} \mid H_1)}{p(\mathbf{r} \mid H_0)}. \tag{41}$$

The likelihood ratio test is:

$$\Lambda(\mathbf{r}) \underset{H_0}{\overset{H_1}{\gtrless}} TH, \tag{42}$$

where the threshold, $TH$, is determined as follows for a fixed $P_f$:

$$P_f = \int_{TH}^{\infty} p(\Lambda \mid H_0)d\Lambda. \tag{43}$$

The joint probability density function of $\mathbf{r}$ is expressed as a product of the marginal probability density functions since all of the noise terms are mutually-uncorrelated, and therefore, statistically-independent

zero-mean Gaussian random variables. The joint probability density function under hypothesis $H_0$ (no satellite signal present) is:

$$p(\mathbf{r} \mid H_0) = \left(\frac{1}{(2\pi)^3 \sigma^6}\right)^K \exp\left(\frac{-|\mathbf{r}|^2}{2\sigma^2}\right). \quad (44)$$

The joint probability density function under hypothesis $H_1$ (satellite signal is present) is:

$$p(\mathbf{r} \mid H_1) = \left[\frac{1}{(2\pi)^3 \sigma^6}\right]^K$$
$$\cdot \exp\left[\frac{-1}{2\sigma^2}\left|\mathbf{r} - \begin{bmatrix} \sqrt{\alpha C}\mathbf{d}_P e^{j\Delta\theta} \\ \sqrt{\beta C}\mathbf{d}_D e^{j\Delta\theta} \\ \sqrt{\gamma C}\mathbf{d}_{C/A}\left(-je^{j\Delta\theta}\right) \end{bmatrix}\right|^2\right]$$
$$= \left[\frac{1}{(2\pi)^3 \sigma^6}\right]^K \exp\left(\frac{-p^2}{2\sigma^2}\right), \quad (45)$$

where:

$$p^2$$
$$= |\mathbf{r}|^2 + KC - 2\sqrt{C}\cos(\Delta\theta)$$
$$\cdot \sum_{k=1}^K \left(\sqrt{\alpha}I_{P,k}d_{P,k} + \sqrt{\beta}I_{D,k}d_{D,k} - \sqrt{\gamma}Q_{C/A,k}d_{C/A,k}\right)$$
$$- 2\sqrt{C}\sin(\Delta\theta)$$
$$\cdot \sum_{k=1}^K \left(\sqrt{\alpha}Q_{P,k}d_{P,k} + \sqrt{\beta}Q_{D,k}d_{D,k} + \sqrt{\gamma}I_{C/A,k}d_{C/A,k}\right).$$

After simplifying, the joint probability density function is now:

$$p(\mathbf{r} \mid H_1) = \left[\frac{1}{(2\pi)^3 \sigma^6}\right]^K \exp\left(\frac{-|\mathbf{r}|^2}{2\sigma^2}\right)\exp\left(\frac{-KC}{2\sigma^2}\right)$$
$$\cdot\exp\left(\frac{\sqrt{C}}{\sigma^2}\cos(\Delta\theta)\sum_{k=1}^K \left(\sqrt{\alpha}I_{P,k}d_{P,k}\right.\right.$$
$$\left.+\sqrt{\beta}I_{D,k}d_{D,k}-\sqrt{\gamma}Q_{C/A,k}d_{C/A,k}\right))$$
$$\cdot\exp\left(\frac{\sqrt{C}}{\sigma^2}\sin(\Delta\theta)\sum_{k=1}^K \left(\sqrt{\alpha}Q_{P,k}d_{P,k}\right.\right.$$
$$\left.+\sqrt{\beta}Q_{D,k}d_{D,k}+\sqrt{\gamma}I_{C/A,k}d_{C/A,k}\right)). \quad (46)$$

Since the carrier phase residual $(\Delta\theta)$, the overlay code bit $(d_P)$, and the data bits $(d_D, d_{C/A})$, are unknown, each is considered a random variable with a known *a priori* density. The conditional probability density functions in the likelihood ratio can be found by averaging $p(\mathbf{r} \mid H_0, \theta, d_P, d_D, d_C)$ and $p(\mathbf{r} \mid H_1, \theta, d_P, d_D, d_C)$ over the probability density function of the random carrier phase residual and the

probability mass function of the random bits:

$$p(\mathbf{r}|H_1) = \sum_{\mathbf{d}_P,\mathbf{d}_D,\mathbf{d}_{C/A}\in\{B\}} p(\mathbf{d}_P,\mathbf{d}_D,\mathbf{d}_{C/A})$$
$$\cdot \int_0^{2\pi} p\left(\mathbf{r}|H_1, \Delta\theta, d_P, d_D, d_{C/A}\right) p\left(\Delta\theta|H_1\right) d\Delta\theta,$$
$$p(\mathbf{r}|H_0) = \sum_{\mathbf{d}_P,\mathbf{d}_D,\mathbf{d}_{C/A}\in\{B\}} p(\mathbf{d}_P,\mathbf{d}_D,\mathbf{d}_{C/A})$$
$$\cdot \int_0^{2\pi} p\left(\mathbf{r}|H_0, \Delta\theta, d_P, d_D, d_{C/A}\right) p\left(\Delta\theta|H_0\right) d\Delta\theta,$$

where $B$ represents all possible combinations of the L1C data, the L1C pilot, and the C/A navigation symbols over the observation interval.

The likelihood ratio is now:

$$\Lambda(\mathbf{r}) = \frac{p\left(\mathbf{r} \mid H_1\right)}{p\left(\mathbf{r} \mid H_0\right)}$$
$$= \sum_{\mathbf{d}_P,\mathbf{d}_D,\mathbf{d}_{C/A}\in\{B\}} p(\mathbf{d}_P,\mathbf{d}_D,\mathbf{d}_{C/A})$$
$$\cdot\frac{1}{2\pi}\int_0^{2\pi}\left[\left[\frac{1}{(2\pi)^6 \sigma^6}\right]^K \exp\left(\frac{-|\mathbf{r}|^2}{2\sigma^2}\right)\exp\left(\frac{-KC}{2\sigma^2}\right)\right.$$
$$\cdot\exp\left(\frac{\sqrt{C}}{\sigma^2}\cos(\Delta\theta)(x)\right)$$
$$\cdot\exp\left(\frac{\sqrt{C}}{\sigma^2}\sin(\Delta\theta)(y)\right)\left((2\pi)^3\sigma^6\right)^K \exp\left(\frac{+|\mathbf{r}|^2}{2\sigma^2}\right)\right]d\Delta\theta$$
$$= \exp\left(\frac{-KC}{2\sigma^2}\right)\sum_{\mathbf{d}_P,\mathbf{d}_D,\mathbf{d}_{C/A}\in\{B\}} p(\mathbf{d}_P,\mathbf{d}_D,\mathbf{d}_{C/A})$$
$$\cdot\frac{1}{2\pi}\int_0^{2\pi}\exp\left(\frac{\sqrt{C}}{\sigma^2}\cos(\Delta\theta)(x)\right)$$
$$\cdot\exp\left(\frac{\sqrt{C}}{\sigma^2}\sin(\Delta\theta)(y)\right)d\Delta\theta, \quad (47)$$

where:

$$x = \sum_{k=1}^K \left(\sqrt{\alpha}I_{P,k}d_{P,k}+\sqrt{\beta}I_{D,k}d_{D,k}-\sqrt{\gamma}Q_{C/A,k}d_{C/A,k}\right),$$
$$y = \sum_{k=1}^K \left(\sqrt{\alpha}Q_{P,k}d_{P,k}+\sqrt{\beta}Q_{D,k}d_{D,k}+\sqrt{\gamma}I_{C/A,k}d_{C/A,k}\right). (48)$$

The first exponential function in (47) is not a function of the observable, the carrier phase offset, or overlay/data bits; thus, the offset is incorporated into the threshold so that the likelihood ratio for the optimal

GPS C/A and L1C joint detector becomes:

$$\Lambda(\mathbf{r})$$

$$= \sum_{\mathbf{d}_P, \mathbf{d}_D, \mathbf{d}_{C/A} \in \{B\}} p(\mathbf{d}_P, \mathbf{d}_D, \mathbf{d}_{C/A})$$

$$\cdot \frac{1}{2\pi} \int_0^{2\pi} \left[ \exp\left( \frac{\sqrt{C}}{\sigma^2} \cos(\Delta\theta)\,(x) \right) \exp\left( \frac{\sqrt{C}}{\sigma^2} \sin(\Delta\theta)\,(y) \right) \right] \mathrm{d}\Delta\theta$$

$$= \sum_{\mathbf{d}_P, \mathbf{d}_D, \mathbf{d}_{C/A} \in \{B\}} p(\mathbf{d}_P, \mathbf{d}_D, \mathbf{d}_{C/A}) I_0\left( \frac{\sqrt{C}}{\sigma^2} \sqrt{x^2 + y^2} \right), \quad (49)$$

where $I_0$ is the modified Bessel function of zeroth order and where $x$ and $y$ are defined in (48).

**REFERENCES**

[1] C. Yang, C. Hegarty, and M. Tran, "Acquisition of the gps l5 signal using coherent combining of i5 and q5," *ION GNSS 17th International Technical Meeting of the Satellite Division*, September 2004.

[2] P. G. Mattos, "Acquisition of the galileo oas l1b/c signal for the mass-market receiver," *ION GNSS 18th International Technical Meeting of the Satellite Division*, 2005.

[3] ——, "Galileo l1c - acquisition complexity: Cross correlation benefits, sensitivity discussions on the choice of pure pilot, seconday code, or something different," *IEEE*, 2006.

[4] C. J. Hegarty, "Optimal and near-optimal detectors for acquisition of the gps l5 signal," *ION National Technical Meeting 2006*, January 2006.

[5] D. Borio, C. O'Driscoll, and G. Lachapelle, "Coherent, noncoherent, and differentially coherent combining techniques for acquisition of new composite gnss signals," *Aerospace and Electronic Systems, IEEE Transactions on*, vol. 45, no. 3, pp. 1227 –1240, july 2009.

[6] F. Macchi-Gernot, M. G. Petovello, and G. Lachapelle, "Combined acquisition and tracking methods for gps l1 c/a and l1c signals," *International Journal of Navigation and Observation*, 2010.

[7] SAIC, *Navstar GPS Space Segment / Navigation User Interfaces, IS-GPS-200E*, Science Applica-

tions International Corporation, El Segundo, CA, June 8, 2010.

[8] ——, "Navstar gps space segment / user segment l1c interface, is-gps-800a," Science Applications International Corporation, Tech. Rep., June 8, 2010.

[9] J. Betz, M. Blanco, C. Cahn, P. Dafesh, C. Hegarty, K. Hudnut, V. Kasemsri, R. Keegan, K. Kovach, L. Lenahan, H. Ma, J. Rushanan, J. Rushanan, D. Sklar, T. Stansell, C. Wang, and S. Yi, "Description of the l1c signal," *Proceedings of the 19th International Technical Meeting of the Satellite Division of The Institute of Navigation (ION GNSS 2006)*, pp. 2080 – 2091, September 2006.

[10] T. Stansell, K. Hudnut, and R. Keegan, "Gps l1c: Enhanced performance, receiver design suggestions, and key contributions," *23rd International Technical Meeting of the Satellite Division of The Institute of Navigation*, 2010.

[11] J. J. Rushanan, "The spreading and overlay codes for the l1c signal," *NAVIGATION: Journal of The Institute of Navigation*, vol. 54, no. 1, pp. 43 – 51, 2007.

[12] J. W. Betz, "Binary offset carrier modulations for radionavigation," *Navigation: Journal of the Institute of Navigation*, vol. 48, no. 4, pp. 227–246, March 2002.

[13] P. Misra and P. Enge, *Global Positioning System: Signals, Measurements and Performance*, revised second edition ed. Lincoln, MA: Ganga-Jamuna Press, 2011.

[14] K. C. Seals, W. R. Michalson, P. F. Swaszek, and R. J. Hartnett, "Analysis of L1C acquisition by combining pilot and data components over multiple code periods," *ION International Technical Meeting 2013*, January 2013.

[15] ——, "Analysis of coherent combining for gps l1c acquisition," *ION GNSS 2012*, September 2012.

[16] H. L. V. Trees, *Detection, Estimation, and Modulation Theory Part I*. Wiley, 1968.

[17] J. G. Proakis, *Digital Communications*. McGraw Hill, 2001.